Zentrum für Technomathematik
Fachbereich 3 – Mathematik und Informatik

A Multi-Mesh Finite Element Method for Phase Field Simulations

Alfred Schmidt

Report 02–03

Berichte aus der Technomathematik

Report 02–03 April 2002

A Multi-Mesh Finite Element Method for Phase Field Simulations

Alfred Schmidt

Zentrum für Technomathematik, Universität Bremen, Germany
schmidt@math.uni-bremen.de

Abstract. In phase field models, different components of the solution (temperature and phase variable) exhibit a strongly different local behaviour. An optimal discretization should use a mesh for each component. We present a general framework for the adaptive solution of coupled systems and its application to phase field simulations.

Free boundary problems give rise to coupled systems of partial differential equations, which are prominent examples of systems where a careful numerical discretization is needed in order to resolve the solution's behaviour. Usually, a high resolution is essential near the free boundary, while coarser meshes are sufficient in the bulk. A reasonable numerical method should use locally adapted meshes to fulfil both the needs of accuracy and efficiency. For coupled systems like the phase field system, where components of the solution show strongly different local behaviour, an optimal discretization should use specially adapted meshes for each component.

1 Models for solidification

An undercooling or oversaturation of a liquid leads to a rapid solidification of the material. Models for this behaviour include energy and/or mass transport by diffusion and/or convection as well as energy/mass conservation conditions across the interface, like the Stefan condition. On a certain (meso-) scale, additional surface effects at the phase boundary play an important role, depending on curvature C or velocity V of the moving interface Γ, usually described by a Gibbs-Thomson relation like

$$\varepsilon_c C_\Gamma + \varepsilon_v V_\Gamma + \theta = 0 \qquad \text{on } \Gamma.$$

Anisotropic surface effects lead to dendritic growth.

Mathematical models for solidification with surface effects differ mainly in the treatment of the free boundary, defining it as a sharp interface, a level set, or a diffuse interface (phase field). Numerical methods for solidification simulations are developed following the same lines.

1.1 Sharp interface models

In a sharp interface model, the phase boundary is a (smooth) hyper-surface of the underlying space (a surface in 3D or a curve in 2D). The advantage of the treatment of the interface as a smooth surface is its lower dimension and that curvature, which appears in the Gibbs-Thomson law, is well defined. Drawbacks are that the standard model allows no changes in interface topology, no nucleation. The notion of varifolds allows for some possibilities in this direction.

The free boundary problem leads to a degenerate parabolic equation for the interface motion, like an anisotropic mean curvature flow equation, coupled with heat or mass diffusion in solid and liquid phases. Additionally, convection can be added by coupling to Navier-Stokes' equations in the time dependent liquid phase.

Numerical methods for sharp interface simulations. The sharp interface model leads to numerical methods with separate discretizations of bulk (3D) and interface (2D) (or 2D & 1D).

In the bulk, a fine mesh is essential near the interface to sufficiently resolve the behaviour of solutions (temperature, concentration). Adaptively refined meshes in finite element methods are crucial to get enough resolution, especially in 3D. A numerical sharp interface finite element method with adaptive meshing in 2D and 3D was presented in [7,8], with additional convection in 2D in [2].

1.2 Diffuse interface models

Phase field models can be formulated either with a double obstacle potential or a smooth double well potential. We want to restrict ourself here to an obstacle formulation, as introduced by Blowey and Elliott [3].

The model describes the evolution of temperature θ and phase variable χ in a domain Ω and is a system of two (degenerate) parabolic equations:

$$\begin{aligned} \partial_t(\theta + \lambda\chi) - \kappa\Delta\theta &= f \\ \varepsilon\,\partial_t\chi - \varepsilon\,\mathrm{div}(a(\nabla\chi)) + \Lambda(\chi) - \tfrac{1}{\varepsilon}\beta\chi &\ni \gamma\theta \end{aligned}$$

in $\Omega \times (0,T)$ plus boundary and initial conditions. The function a may include anisotropic solidification parameters, and Λ is a (set valued) maximal monotone graph, the subdifferential of the double obstacle potential,

$$\Lambda(s) = \begin{cases} (-\infty, 0] & \text{if } s = -1 \\ 0 & \text{if } s \in (-1,1) \\ [0, +\infty) & \text{if } s = +1 \end{cases}$$

with the effect that values of χ are in the interval $[-1,+1]$. f is a given heat source density, λ, κ, and β are non-negative, material-dependent coefficients,

and $\varepsilon > 0$ a small parameter. The phase variable χ is equal to -1 (solid) or $+1$ (liquid) everywhere but in a narrow transition region of width $O(\varepsilon)$. For $\varepsilon \to 0$, the solution converges against a solution of the sharp interface model with a corresponding Gibbs-Thomson relation. Figure 1 shows the evolution of the phase boundary during the solidification of an undercooled liquid.

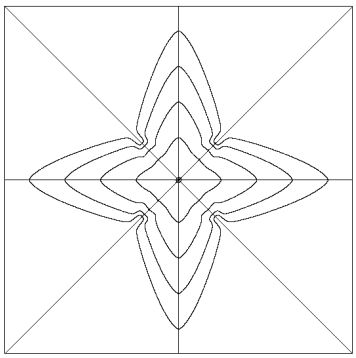

Fig. 1. Solid-liquid interface at different times

Both components of the solution, temperature and phase variable, show a strongly different local behaviour, see Figure 2.

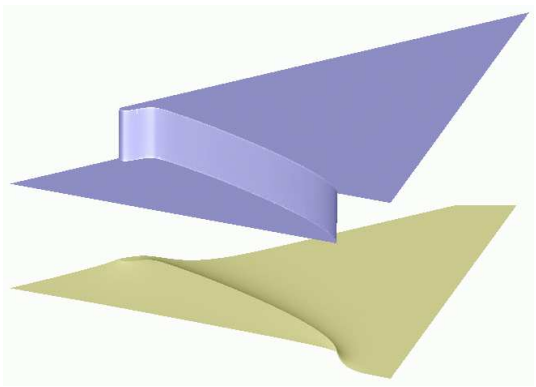

Fig. 2. Graphs of phase variable and temperature on 1/8 domain

- The phase variable is constant outside of a moving narrow strip of width $O(\varepsilon)$, where the phase transition occurs. Here, $|\nabla\chi| = O(\varepsilon^{-1})$.
- The temperature satisfies the heat equation outside this strip, thus it is smooth. Inside the moving strip, the gradient of temperature changes

rapidly. In the limit $\varepsilon \to 0$, the Stefan condition holds at the sharp interface,

$$(\kappa \nabla \theta_{\text{liquid}} - \kappa \nabla \theta_{\text{solid}}) \cdot n = -\lambda V.$$

In order to resolve this behaviour with a finite element approximation, different requirements to the discretization hold for both components.

- The mesh for discretization of χ must have a local mesh width of $h_S < c\varepsilon$. Outside this strip, where χ is constant, the mesh might be arbitrarily coarse. In order to be able to track nucleations, the phase field system should be solved in the whole domain, not only near the current interface.
- To resolve the temperature behaviour, a much coarser mesh is sufficient in the strip than is needed for the phase variable. On the other hand, the mesh must have a sufficient fineness also in the rest of the domain.

A separate discretization for both temperature and phase variable is needed in order to meet all requirements in an efficient numerical method.

2 Adaptive finite element methods for coupled systems of PDE

Besides phase transitions, many physical problems lead to coupled systems of partial differential equations, too. Especially in case of nonlinear phenomena, the components u_i, $i = 1, \ldots, n$ may show a strongly different behaviour (smoothness of solutions etc.) in the common underlying domain $\Omega \subset \mathbb{R}^d$.

The usual adaptive discretization for systems of PDEs uses the same mesh for all components, locally refined based on a posteriori error indicators for the sum of error contributions on each mesh element.

An optimal adaptive discretization should use different locally refined meshes for different components of the solution, controled by separate error indicators for each component.

In [6] we present a general concept for adaptive finite element methods for stationary or time dependent coupled problems.

Solution components u_i are discretized in finite element spaces X_i, which are based on different locally refined simplicial grids $\mathcal{S}_i$, where all meshes $\mathcal{S}_i$ are refinements of the same macro triangulation $\mathcal{S}_0$ of Ω, see Figure 3 for a simple example.

The advantages of this approach are

- separately adapted mesh for each component of the solution;
- altogether less degrees of freedom, thus more efficient;
- by the common macro mesh, a direct local hierarchy of the triangulations $\mathcal{S}_i$ is given. This enables an *exact* evaluation of each other component U_j on the elements of mesh $\mathcal{S}_i$.

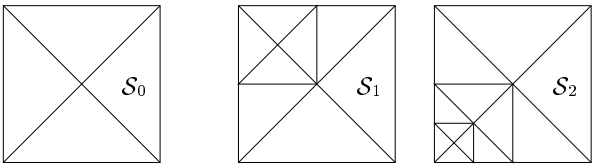

Fig. 3. Two different refinements of a macro triangulation $\mathcal{S}_0$

A somewhat similar idea for phase field simulations was proposed by Elliott and Gardiner [5], who use two separate meshes for temperature and phase variable. A fine mesh with mesh size $h \ll \varepsilon$ for the phase variable is used only near the transition region (selected by a 'mask'), a coarse mesh with mesh size $H = 4h$ for the temperature. Use of the 'mask' reduces computations for the phase variable significantly, but does not allow to track nucleations, e. g. Both meshes are aligned, but no error estimators or local mesh refinements are used.

2.1 Aspects of implementation

The adaptive multi-mesh method is implemented in the finite element toolbox ALBERT, a joint development with K. G. Siebert [9,10]. The toolbox uses simplicial meshes in 2D (triangles) and 3D (tetrahedra) and local refinement by bisection of elements, which induces a hierarchical structure of meshes and finite element spaces.

The multi-mesh concept introduces the traversal of a common, *virtually refined* mesh $\mathcal{S}_M$, see Figure 4, for calculation of coupling terms, which involve several components or functions from finite element spaces defined on different meshes, like $\int_\Omega U_i \Phi$ with $U_i \in X_i$, $\Phi \in X_j$.

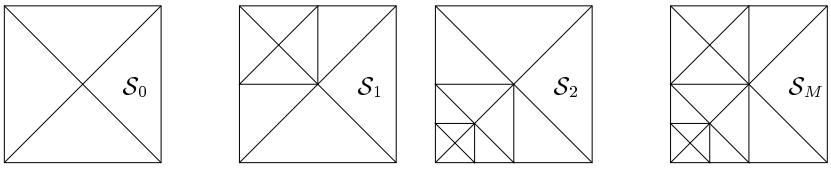

Fig. 4. Virtual mesh $\mathcal{S}_M$ with locally maximal refinement from $\mathcal{S}_1, \mathcal{S}_2$

2.2 Numerical analysis and adaptive methods

We recall the standard a posteriori error estimates and adaptive finite element methods for a scalar elliptic problem. The error $\|u-U\|$ between the solution u

and a discrete approximation U is estimated by a sum of local error indicators, e. g.

$$\|u - U\|^2 \leq \sum_{S \in \mathcal{S}} \eta_S^2,$$

where the indicators η_S must be computable from the discrete solution U and given data of the problem (*a posteriori*).

On an quasi-optimal mesh for a given error tolerance *tol*, the local error indicators are equally distributed over all mesh elements,

$$\eta_S^2 \approx \frac{tol^2}{\#\mathcal{S}} \qquad \text{for all } S \in \mathcal{S},$$

compare [1], e. g. A similar approach is used in case of coupled systems. The goal is an estimate of the errors $\|u_i - U_i\|$ by a sum of local error indicators on separate meshes, like

$$\sum_{i=1}^{n} \|u_i - U_i\|^2 \leq \sum_{S \in \mathcal{S}_1} \eta_{1,S}^2 + \cdots + \sum_{S \in \mathcal{S}_n} \eta_{n,S}^2.$$

In order to describe a quasi-optimal set of meshes, one possibility is to split the total tolerance *tol* to the separate meshes

$$tol_1^2 + \cdots + tol_n^2 = tol^2$$

and optimize every single mesh. This leads to decoupled equidistribution conditions

$$\eta_{i,S}^2 \approx \frac{tol_i^2}{\#\mathcal{S}_i} \quad \text{for all } S \in \mathcal{S}_i, i = 1, \ldots, n.$$

3 Adaptive method for phase field models

In a joint paper with Z. Chen and R.H. Nochetto [4], we derive error estimates and adaptive methods for the double obstacle phase field system. Denoting by $u = \theta + \lambda\chi$ the energy density, and again discrete (finite element) functions by uppercase letters, the estimate looks like

$$\begin{aligned} &\|u - U\|_{L^\infty(0,T;H^{-1}(\Omega))} + \sqrt{\varepsilon}\|\chi - X\|_{L^\infty(0,T;L^2(\Omega))} \\ &\quad + \left(\int_0^T \|\theta - \Theta\|_{L^2(\Omega)}^2 + \alpha\varepsilon \, \|\nabla\chi - \nabla X\|_{L^2(\Omega)}^2 \, dt \right)^{1/2} \\ &\leq \text{computable terms, localizable to mesh elements.} \end{aligned}$$

In [4], we use a common mesh for the discretization of temperature and phase variable. The local error indicators η_S contain contributions from both components,

$$\text{Estimated error } \leq \eta_0 + \max_m \sum_{S \in \mathcal{S}^m} \eta_S^2,$$

where m is the time step index. A quasi-optimal common mesh fulfils the equidistribution condition for the local indicators

$$\eta_S^2 \approx \frac{tol^2}{\#\mathcal{S}^m} \quad \text{for all } S \in \mathcal{S}^m.$$

Here, the total mesh element count $\#\mathcal{S}^m$ is very large because of the fine resolution in the strip, thus the local temperature error must be very small also in elements far from the interface.

Adaptive FE method with separate meshes

A separation of contributions from temperature and phase variable in the error indicator is possible:

$$\text{Estimated error } \leq \eta_0 + \max_m \Big(\sum_{S \in \mathcal{S}_\theta^m} \eta_{\theta,S}^2 + \sum_{S \in \mathcal{S}_\chi^m} \eta_{\chi,S}^2 \Big).$$

A split of the tolerance to both meshes, as described above, leads to a smaller element count $\#\mathcal{S}_\theta^m$, thus larger local error tolerances for the temperature error. It follows that the temperature mesh contains much less elements than a common mesh. Also the mesh for the phase variable contains less elements, as a fine resolution is needed only in the transition region. Figure 5 shows element counts over time. A time-dependent tolerance was used for the error in each time step, which reflects the fact that the interface length grows during the simulation.

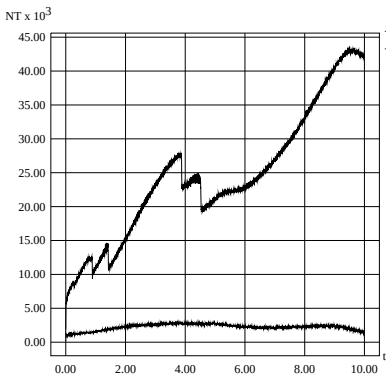

Fig. 5. Element counts for phase variable and temperature meshes over time

Figures 6 and 7 show the temperature and phase variable meshes with zooms to the interface region. Finally, we present in Figures 8-10 a comparison of temperature and phase variable meshes from simulations with three different error tolerances *tol*.

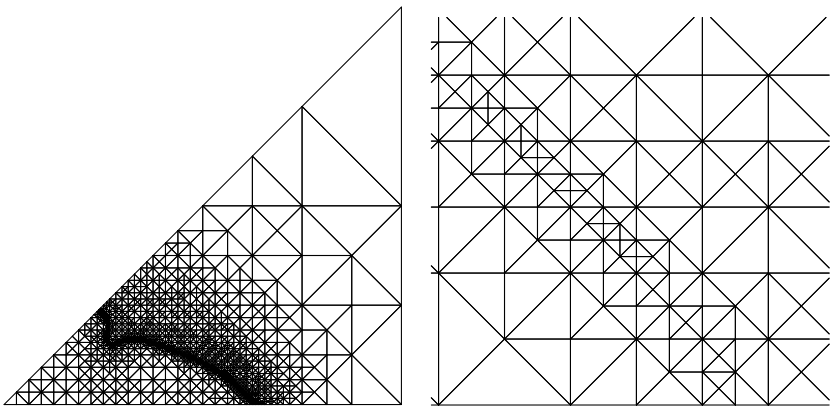

Fig. 6. Temperature mesh (2608 elements) and zoom to interface

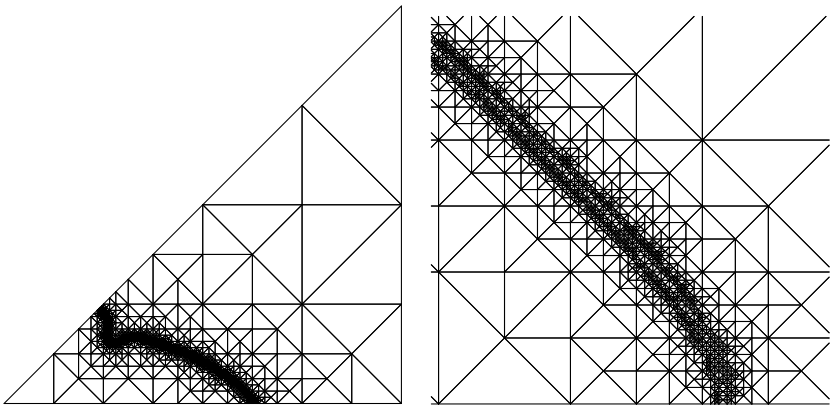

Fig. 7. Phase variable mesh (23015 elements) and zoom

Conclusion

We described an efficient adaptive finite element method for phase field calculations, together with some 2D simulation results. A more detailed description of the multi-mesh method and results from 3D simulations will be presented in forthcoming articles.

Acknowledgements.

This article reports partly joint work with Z. Chen (Beijing), R. H. Nochetto (College Park), and K. G. Siebert (Freiburg).

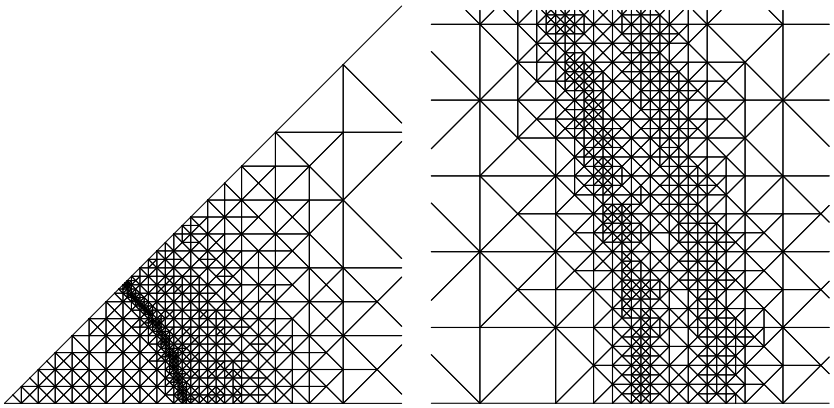

Fig. 8. tol=10: Meshes with 1122 resp. 7440 elements

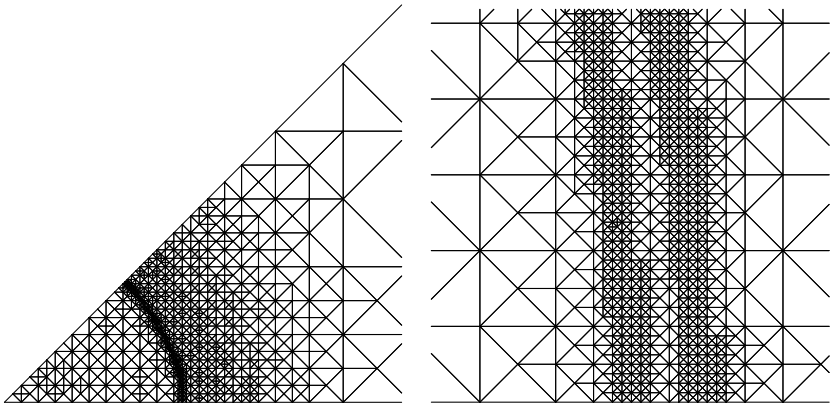

Fig. 9. tol=7: Meshes with 1568 resp. 11813 elements

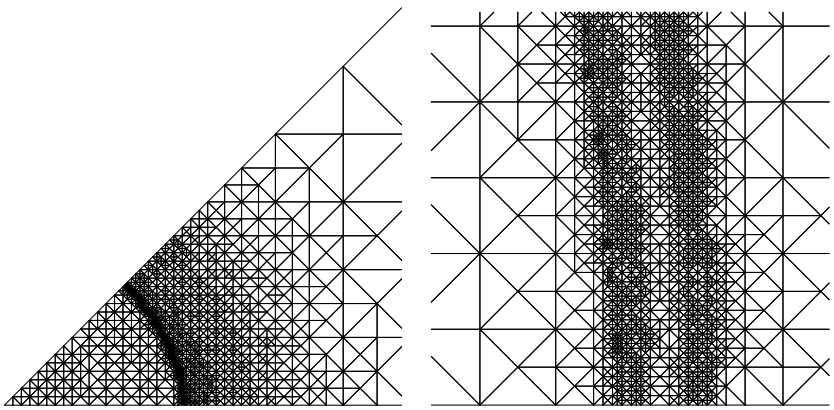

Fig. 10. tol=5: Meshes with 2245 resp. 20631 elements

References

1. I. Babuška and W. Rheinboldt, *Error estimates for adaptive finite element computations*, SIAM J. Numer. Anal., 15 (1978), pp. 736–754.
2. E. Bänsch and A. Schmidt, *Simulation of dendritic crystal growth with thermal convection*, Interfaces and Free Boundaries, 2 (2000), pp. 95–115.
3. J. Blowey and C. Elliott, *Curvature dependent phase boundary motion and parabolic double obstacle problems.*, in Ni, Wei-Ming (ed.) et al., Degenerate diffusions. IMA Vol. Math. Appl. 47, 19-60 , 1993.
4. Z. Chen, R. H. Nochetto, and A. Schmidt, *Adaptive finite element methods for diffuse interface models.* In preparation.
5. C. Elliott and A. Gardiner, *Double obstacle phase field computations of dendritic growth.* Report 96/19, University of Sussex.
6. A. Schmidt, *Adaptive methods for coupled systems.* In preparation.
7. ———, *Computation of three dimensional dendrites with finite elements*, J. Comput. Phys., 125 (1996), pp. 293–312.
8. ———, *Approximation of crystalline dendrite growth in two space dimensions*, Acta Math. Univ. Comenianae, 67 (1998), pp. 57–68.
9. A. Schmidt and K. G. Siebert, *ALBERT: An adaptive hierarchical finite element toolbox.* Preprint 06/2000 Freiburg, 2000. Documentation.
10. ———, *ALBERT – Software for scientific computations and applications*, Acta Math. Univ. Comenianae., 70 (2001), pp. 105–122.

Berichte aus der Technomathematik ISSN 1435-7968

`http://www.math.uni-bremen.de/zetem/berichte.html`

— Vertrieb durch den Autor —

Reports **Stand: 26. April 2002**

98–01. Peter Benner, Heike Faßbender:
An Implicitly Restarted Symplectic Lanczos Method for the Symplectic Eigenvalue Problem, Juli 1998.

98–02. Heike Faßbender:
Sliding Window Schemes for Discrete Least-Squares Approximation by Trigonometric Polynomials, Juli 1998.

98–03. Peter Benner, Maribel Castillo, Enrique S. Quintana-Ortí:
Parallel Partial Stabilizing Algorithms for Large Linear Control Systems, Juli 1998.

98–04. Peter Benner:
Computational Methods for Linear–Quadratic Optimization, August 1998.

98–05. Peter Benner, Ralph Byers, Enrique S. Quintana-Ortí, Gregorio Quintana-Ortí:
Solving Algebraic Riccati Equations on Parallel Computers Using Newton's Method with Exact Line Search, August 1998.

98–06. Lars Grüne, Fabian Wirth:
On the rate of convergence of infinite horizon discounted optimal value functions, November 1998.

98–07. Peter Benner, Volker Mehrmann, Hongguo Xu:
A Note on the Numerical Solution of Complex Hamiltonian and Skew-Hamiltonian Eigenvalue Problems, November 1998.

98–08. Eberhard Bänsch, Burkhard Höhn:
Numerical simulation of a silicon floating zone with a free capillary surface, Dezember 1998.

99–01. Heike Faßbender:
The Parameterized SR Algorithm for Symplectic (Butterfly) Matrices, Februar 1999.

99–02. Heike Faßbender:
Error Analysis of the symplectic Lanczos Method for the symplectic Eigenvalue Problem, März 1999.

99–03. Eberhard Bänsch, Alfred Schmidt:
Simulation of dendritic crystal growth with thermal convection, März 1999.

99–04. Eberhard Bänsch:
Finite element discretization of the Navier-Stokes equations with a free capillary surface, März 1999.

99–05. Peter Benner:
Mathematik in der Berufspraxis, Juli 1999.

99–06. Andrew D.B. Paice, Fabian R. Wirth:
Robustness of nonlinear systems and their domains of attraction, August 1999.

99–07. Peter Benner, Enrique S. Quintana-Ortí, Gregorio Quintana-Ortí:
Balanced Truncation Model Reduction of Large-Scale Dense Systems on Parallel Computers, September 1999.

99–08. Ronald Stöver:
Collocation methods for solving linear differential-algebraic boundary value problems, September 1999.

99–09. Huseyin Akcay:
Modelling with Orthonormal Basis Functions, September 1999.

99–10. Heike Faßbender, D. Steven Mackey, Niloufer Mackey:
Hamilton and Jacobi come full circle: Jacobi algorithms for structured Hamiltonian eigenproblems, Oktober 1999.

99–11. Peter Benner, Vincente Hernández, Antonio Pastor:
On the Kleinman Iteration for Nonstabilizable System, Oktober 1999.

99–12. Peter Benner, Heike Faßbender:
A Hybrid Method for the Numerical Solution of Discrete-Time Algebraic Riccati Equations, November 1999.

99–13. Peter Benner, Enrique S. Quintana-Ortí, Gregorio Quintana-Ortí:
Numerical Solution of Schur Stable Linear Matrix Equations on Multicomputers, November 1999.

99–14. Eberhard Bänsch, Karol Mikula:
Adaptivity in 3D Image Processing, Dezember 1999.

00–01. Peter Benner, Volker Mehrmann, Hongguo Xu:
Perturbation Analysis for the Eigenvalue Problem of a Formal Product of Matrices, Januar 2000.

00–02. Ziping Huang:
Finite Element Method for Mixed Problems with Penalty, Januar 2000.

00–03. Gianfrancesco Martinico:
Recursive mesh refinement in 3D, Februar 2000.

00–04. Eberhard Bänsch, Christoph Egbers, Oliver Meincke, Nicoleta Scurtu:
Taylor-Couette System with Asymmetric Boundary Conditions, Februar 2000.

00–05. Peter Benner:
Symplectic Balancing of Hamiltonian Matrices, Februar 2000.

00–06. Fabio Camilli, Lars Grüne, Fabian Wirth:
A regularization of Zubov's equation for robust domains of attraction, März 2000.

00–07. Michael Wolff, Eberhard Bänsch, Michael Böhm, Dominic Davis:
Modellierung der Abkühlung von Stahlbrammen, März 2000.

00–08. Stephan Dahlke, Peter Maaß, Gerd Teschke:
Interpolating Scaling Functions with Duals, April 2000.

00–09. Jochen Behrens, Fabian Wirth:
A globalization procedure for locally stabilizing controllers, Mai 2000.

00–10. Peter Maaß, Gerd Teschke, Werner Willmann, Günter Wollmann:
Detection and Classification of Material Attributes – A Practical Application of Wavelet Analysis, Mai 2000.

00–11. Stefan Boschert, Alfred Schmidt, Kunibert G. Siebert, Eberhard Bänsch, Klaus-Werner Benz, Gerhard Dziuk, Thomas Kaiser:
Simulation of Industrial Crystal Growth by the Vertical Bridgman Method, Mai 2000.

00–12. Volker Lehmann, Gerd Teschke:
Wavelet Based Methods for Improved Wind Profiler Signal Processing, Mai 2000.

00–13. Stephan Dahlke, Peter Maass:
A Note on Interpolating Scaling Functions, August 2000.

00–14. Ronny Ramlau, Rolf Clackdoyle, Frédéric Noo, Girish Bal:
Accurate Attenuation Correction in SPECT Imaging using Optimization of Bilinear Functions and Assuming an Unknown Spatially-Varying Attenuation Distribution, September 2000.

00–15. Peter Kunkel, Ronald Stöver:
Symmetric collocation methods for linear differential-algebraic boundary value problems, September 2000.

00–16. Fabian Wirth:
The generalized spectral radius and extremal norms, Oktober 2000.

00–17. Frank Stenger, Ahmad Reza Naghsh-Nilchi, Jenny Niebsch, Ronny Ramlau:
A unified approach to the approximate solution of PDE, November 2000.

00–18. Peter Benner, Enrique S. Quintana-Ortí, Gregorio Quintana-Ortí:
Parallel algorithms for model reduction of discrete–time systems, Dezember 2000.

00–19. Ronny Ramlau:
A steepest descent algorithm for the global minimization of Tikhonov–Phillips functional, Dezember 2000.

01–01. Efficient methods in hyperthermia treatment planning:
Torsten Köhler, Peter Maass, Peter Wust, Martin Seebass, Januar 2001.

01–02. Parallel Algorithms for LQ Optimal Control of Discrete-Time Periodic Linear Systems:
Peter Benner, Ralph Byers, Rafael Mayo, Enrique S. Quintana-Ortí, Vicente Hernández, Februar 2001.

01–03. Peter Benner, Enrique S. Quintana-Ortí, Gregorio Quintana-Ortí:
Efficient Numerical Algorithms for Balanced Stochastic Truncation, März 2001.

01–04. Peter Benner, Maribel Castillo, Enrique S. Quintana-Ortí:
Partial Stabilization of Large-Scale Discrete-Time Linear Control Systems, März 2001.

01–05. Stephan Dahlke:
Besov Regularity for Edge Singularities in Polyhedral Domains, Mai 2001.

01–06. Fabian Wirth:
A linearization principle for robustness with respect to time-varying perturbations, Mai 2001.

01–07. Stephan Dahlke, Wolfgang Dahmen, Karsten Urban:
Adaptive Wavelet Methods for Saddle Point Problems - Optimal Convergence Rates, Juli 2001.

01–08. Ronny Ramlau:
Morozov's Discrepancy Principle for Tikhonov regularization of nonlinear operators, Juli 2001.

01–09. Michael Wolff:
Einführung des Drucks für die instationären Stokes–Gleichungen mittels der Methode von Kaplan, Juli 2001.

01–10. Stephan Dahlke, Peter Maaß, Gerd Teschke:
Reconstruction of Reflectivity Desities by Wavelet Transforms, August 2001.

01–11. Stephan Dahlke:
Besov Regularity for the Neumann Problem, August 2001.

01–12. Bernard Haasdonk, Mario Ohlberger, Martin Rumpf, Alfred Schmidt, Kunibert G. Siebert:
h–p–Multiresolution Visualization of Adaptive Finite Element Simulations, Oktober 2001.

01–13. Stephan Dahlke, Gabriele Steidl, Gerd Teschke:
Coorbit Spaces and Banach Frames on Homogeneous Spaces with Applications to Analyzing Functions on Spheres, August 2001.

02–01. Michael Wolff, Michael Böhm:
Zur Modellierung der Thermoelasto-Plastizität mit Phasenumwandlungen bei Stählen sowie der Umwandlungsplastizität, Februar 2002.

02–02. Stephan Dahlke, Peter Maaß:
An Outline of Adaptive Wavelet Galerkin Methods for Tikhonov Regularization of Inverse Parabolic Problems, April 2002.

02–03. Alfred Schmidt:
A Multi-Mesh Finite Element Method for Phase Field Simulations, April 2002.